2009 American Control Conference
Hyatt Regency Riverfront, St. Louis, MO, USA
June 10-12, 2009

Nonlinear Multivariable Predictive Control of an Autothermal Reforming Reactor for Fuel Cell Applications

Yongyou Hu and Donald J. Chmielewski

Abstract—**In this work, we present a computationally efficient nonlinear multivariable predictive controller (NMPC) for an autothermal reforming (ATR) reactor. The proposed NMPC scheme is based on a fast reduced order nonlinear model and consists of three parts. The first is a steady state optimizer, which aims to minimize fuel flow for a given hydrogen demand while simultaneously observing the lower bound on the reactor temperature to maintain ignition of the reactor. The second part of the controller is to find a desired input/output trajectory via an offline nonlinear dynamic optimization problem subject to process constraints. The third portion of the controller employs a linearized model around the trajectory and minimizes an unconstrained trajectory tracking problem of which analytic solution is obtained. A linear Kalman Filter (KF) is employed to estimate process states. The proposed NMPC is compared with the classic feed-forward controller to illustrate improved performance.**

I. Introduction

As a promising hydrogen delivery technology for fuel cell vehicles, autothermal reforming of hydrocarbon fuels has attracted significant research interest [1-5]. Experimental and simulation-based studies have revealed that during start-up and load changes tight control of the ATR reactor is vital for catalyst protection and maintaining ignition of the reactor. Recent efforts on controller design for reforming reactors include [6-7]. However, these efforts are mainly focused on controller design for Catalytic Partial Oxidation (CPOX) reactors where only fuel and air are fed into the reactor and the H_2/CO ratio is comparatively low. In previous work, we investigated the classic methods for control of the ATR reactor where CPOX mode is initially operated to preheat the catalyst and then steam/water is injected (named ATR mode) to improve the H_2/CO ratio [8]. It was found that the classic methods could not regulate well the catalyst temperature during the transition from CPOX mode to ATR mode and during large load changes. It was concluded that advanced control (e.g., model predictive control) should be used to address these operating scenarios.

Model predictive control (MPC) has been a staple of the process industries [9-10]. The fundamental principle behind MPC is that it calculates a series of control moves with the available measurements at every time step to optimize future plant behavior as predicted by a process model. Due to its unique advantages in handling process constraints, linear MPC has been widely applied in the process industry (over 4500 commercial applications were reported in [9]).

Many chemical processes are, however, inherently nonlinear. In these cases, nonlinear models are desired to describe the process dynamics within a nonlinear model predictive controller (NMPC) [10-11]. The excessive computational cost, however, remains a major hurdle. Developing computationally efficient NMPC techniques has been the focus of NMPC research field during the past decade [11-14].

A major feature of the ATR reactor is that it is a very fast nonlinear process (the settling time is only around 10 seconds), which makes online implementation more difficult. Currently, there are no references available in the literature regarding advanced control of the ATR reactor. The main objective of this work is to propose and evaluate a KF-based NMPC for the ATR reactor.

II. Process Description

The current effort is just one component of a larger project aimed at identifying the start-up capabilities of a fuel processing unit [15]. This project (titled the Feasibility of Acceptable Start-Time Experimental Reformer [FASTER] project) was charged with constructing a 10 kWe system and showing that it could be started in less than 60 seconds. At the heart of the FASTER process, is the autothermal reforming (ATR) reactor, depicted in figure 1. Within this reactor, it is sufficient to assume that three non-elementary reactions take place [5]:

Total Oxidation:

$$C_mH_n + (m + n/4)O_2 \rightarrow mCO_2 + n/2H_2O \quad (1)$$

Steam Reforming:

$$C_mH_n + mH_2O \rightarrow mCO + (m + n/2)H_2 \quad (2)$$

Water-Gas Shift:

$$CO + H_2O \leftrightarrow CO_2 + H_2 \quad (3)$$

The set of inputs includes the inlet flow rates of air, fuel and steam as well as the temperature of this inlet gas stream. The inlet temperature will depend heavily on the state of the recuperating heat exchanger on the upstream air flow, so it will be treated as a measured disturbance. The air, fuel and steam flows will be the manipulated variables (MVs). Concerning measurable outputs, the set of outputs is limited

Yongyou Hu is with the Chemical and Biological Engineering Department, Illinois Institute of Technology, Chicago, IL 60616 USA (e-mail: huyongy@ iit.edu).

Donald J. Chmielewski is with the Chemical and Biological Engineering Department, Illinois Institute of Technology, Chicago, IL 60616 USA (corresponding author, phone: 312-567-3537; fax: 312-567-8874; e-mail: chmielewski@ iit.edu).

978-1-4244-4524-0/09/$25.00 ©2009 AACC

to four thermocouples on the solid catalyst support at various axial locations, see figure 1. These measurements are at the following locations: 0.08 cm, 0.7 cm, 1.9 cm and 3.1 cm (indicated by T_1, T_2, T_3 and T_4, respectively). In the analysis and model validation of [5], exit concentration of CO and H_2 were utilized. However, in a production scale system the availability of these measurements, including T_1, is unlikely and thus will be ignored in the current study. The selected controlled variable (CV) is T_2, which is the measured temperature with smallest time delay. The non-measurement (system) noise is mainly from the fluctuations in the reactor temperature due to radial non-uniformities. Compared with the temperature fluctuations, the measurement (sensor) noise is much smaller and thus neglected.

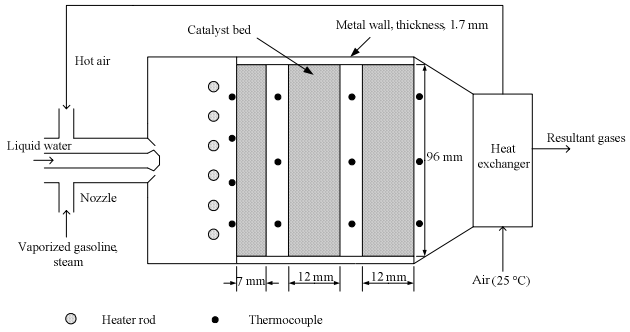

Figure 1: Schematic of the ATR reactor

III. Steady State Optimization

It is reported that fuel cost is up to 68% of the total cost for hydrogen production [16]. In this work, we propose an analytical method to calculate the required minimum fuel flow rate and the corresponding air and steam flow rates for given hydrogen demand.

For ATR mode at steady state, the fuel should be completely consumed within the reactor and it is reasonable to assume that WGS reaches equilibrium at the exit of the reactor [5]. The resulting material and energy balances are given by

$$\dot{m}\hat{c}_{pg}(T_L^{(g)} - T_0^{(g)}) = \frac{F_{O_2}(-\Delta_r H_1)}{(m+n/4)M_{O_2}} + \left\{\frac{F_{fuel}}{M_{C_mH_n}} - \frac{F_{O_2}}{(m+n/4)M_{O_2}}\right\}(-\Delta_r H_2) + \xi(-\Delta_r H_3) \quad (4)$$

$$\frac{(N_{CO} - \xi)(N_{H_2O} - \xi)}{(N_{CO_2} + \xi)(N_{H_2} + \xi)} = \frac{1}{Ke(T_L^{(g)})} \quad (5)$$

where $\hat{c}_{pg}$ is the heat capacity, ξ represents the conversion of WGS and N_i denote the molar flows. For given feed rates, the exit temperature, $T_L^{(g)}$, and WGS conversion, ξ, will be determined easily from equations (4) and (5).

The material balance for hydrogen at steady state leads to

$$\dot{m}_{H_2} = (m+0.5n)\frac{M_{H_2}F_{fuel}}{M_{C_mH_n}} - \frac{(m+0.5n)M_{H_2}F_{O_2}}{(m+0.25n)M_{O_2}} + \xi \cdot M_{H_2} \quad (6)$$

It is well known that low temperature favors the exothermic WGS but may extinguish the reactor or result in unconsumed fuel at the exit. The solution of the NLP reveals that the lower bound on solid temperature is the only active constraint, if the feed rate constraints are not violated. Table 1 shows the optimal results for different hydrogen yields. The inlet conditions in this table will be used as the set points for all subsequent flow controllers.

Table 1 Optimized feed rates for different hydrogen yields (T_{in} = 450 °C)

H2 yield, mol/min	T^l, °C	Fuel, g/min	Air, dm^3/min	Water, g/min	Net H_2 yield*, %
3	800	24.3	93.7	158.6	83.8
	750	22.9	82.75	162.8	86.6
5	800	40.53	156.2	264.3	83.8
	750	38.2	137.9	271.3	86.6
8	800	64.85	250	422.8	83.8
	750	61.0	220.7	434	86.6

* The net H_2 yield is defined by the ratio of H_2 yield to the maximum theoretical H_2 yield when the resultants include only carbon dioxide and hydrogen.

IV. Reference Trajectory Calculation

The reference trajectories for input and output play an important role in MPC technology because they represent the trajectories on which the system gradually reaches the desired set points. Typically the output trajectory is formulated by drawing a first or second order curve from the current value of the control variable (CV) to the new setpoint, with adjustable response speed [9]. A popular approach is to specify the output trajectory, y_d, to be the filtered set point as follows [17]:

$$y_d(k+j) = \alpha^j y_d(k) + (1-\alpha^j) y_{sp}(k),\ j = 1,2,\cdots,P \quad (7)$$

where $0 \le \alpha \le 1$; P is prediction horizon. For ATR control, such gradual transitions should not violate the temperature and flowrate bounds. Thus, the goal of the reference trajectory calculation is to find the feasible input and output trajectories on which the solid temperature (T_2) should approach the desired set point. In order to speed up the NLP problem solution time, a fast reduced order nonlinear dynamic mode has been developed.

A. Reduced Order Model Development

The reduced order model was derived from a kinetic model developed in [5]. The kinetic model was solved via Finite Element Methods (FEM) and validated by experimental data. However, solution via FEM is far too slow to be applied within model based optimization (6 seconds is required for a simulation horizon of 10 seconds).

Our first step to model reduction was to apply the Galerkin method to approximate the temperature profile by a linear combination of basis functions. As a result, the PDEs of the energy balance were reduced to ODEs. This first reduced order model (ROM1) used an ODE solver to solve the mass balance. ROM1 showed significant agreement with the FEM model in terms of temperature and concentration profiles.

The computational cost was reduced from 6 seconds to 1.7 seconds. Our second effort was to approximate the reaction rates by exponential functions and thus to find analytic expression for the concentration profiles. The second reduced order model (ROM2) consisted of ODEs and algebraic equations only:

$$\frac{dx}{dt} = Ax + \hat{q}(x,u,g) \qquad y = Cx \tag{8}$$

where $x = [x_1^{(s)}, x_2^{(s)} \cdots x_N^{(s)}, x_1^{(w)}, x_2^{(w)} \cdots x_N^{(w)}]^T$ is a vector of basis function coefficients; $u = [F_{fuel}, F_{air}, F_{H_2O}]^T$; $g = T_0^{(g)}$, the inlet temperature of the gas and $y = [T_2\ T_3\ T_4]^T$.

The discrete version of the linear state-space model represented by equation (8) is given by

$$x_{k+1} = A_d x_k + \hat{q}_d(x_k, u_k, g_k) \qquad y_k = Cx_k \tag{9}$$

where $A_d = e^{A\cdot\Delta T_s}$ and $\hat{q}_d(x_k,u_k,g_k) = A_d \int_0^{\Delta T_s} e^{-A\tau} d\tau\, \hat{q}(x_k,u_k,g_k)$

It should be noted that we assume $\hat{q}$ is held constant over the sample interval, ΔT_s. This can be thought of as a variation of the traditional sample and hold discretization for linear systems. The developed ROM2 of equation (9) required only 0.002 seconds for a simulation horizon of 10 seconds, and possessed fidelity comparable to ROM1 and the FEM model [14]. Hence, ROM2 was used in the following reference trajectory calculation.

B. The Reference Trajectory Calculation

The NLP problem for trajectory calculation is:

$$\begin{aligned} \min_{\{u_r, y_r, s\}}\ & J = \sum_{k=1}^{P} \beta (y_{r,k} - y_{d,k})^2 + \sum_{j=1}^{3} \gamma^j (u_{r,k}^j - u_s^j)^2 + w \cdot s_k^2 \\ s.t.\ & x_{k+1} = A_d x_k + \hat{q}_d(x_k, u_{r,k}^j, g_k) \\ & y_{r,k} = Cx_k \\ & T^l - s_k \le y_{r,k} \le T^u + s_k, \quad u_r^{l,j} \le u_{r,k}^j \le u_r^{u,j} \\ & \Delta u_{r,k}^j = u_{r,k+1}^j - u_{r,k}^j, \quad \left|\Delta u_{r,k}^j\right| \le \varepsilon^j \end{aligned} \tag{10}$$

where $y_{d,k} = y_d(t=k)$ is the designated temperature reference represented by equation (7), u_s^j are the setpoints for fuel, air and steam flow rates determined from table 1; $y_{r,k} = y_r(t=k)$, $u_{r,k}^j = u_r^j(t=k)$ are the to be determined reference trajectories; s_k is a slack variable vector used to avoid the infeasible solutions due to hard temperature constraints and β, γ^j, w are weighting constants.

Figure 2 shows the calculated input and output trajectories for a transition from CPOX mode (F_{fuel} = 30 g/min, F_{air} =60 dm^3/min, F_{water} = 0 g/min) to ATR mode (F_{fuel} = 38.2 g/min, F_{air}= 137.9 dm^3/min, F_{water}= 271.3 g/min). The optimal trajectories for all three feed flow rates are basically in the ramp formulation and the changes within each sampling time are limited by $\Delta u_{\max}^j$ (see the top plot of figure 2). If we apply those input trajectories to ROM1, we find only minor differences in the temperature trajectories, as shown in the middle plot of figure 2. However, compared with the desired trajectory defined by equation (7) the calculated output trajectory shows significant difference due to the constraints on $\Delta u_{r,k}^j$. Looking at the bottom plot of figure 2, hydrogen flow quickly moves from 1 to 5 mol/min, and the trajectories from different models show only a small difference.

The time required to solve problem (10) is typically around 60 seconds for P = 20, which is significantly larger than the sampling time of the ATR reactor, typically less than 1 second (e.g., ΔT_s =0.5s).

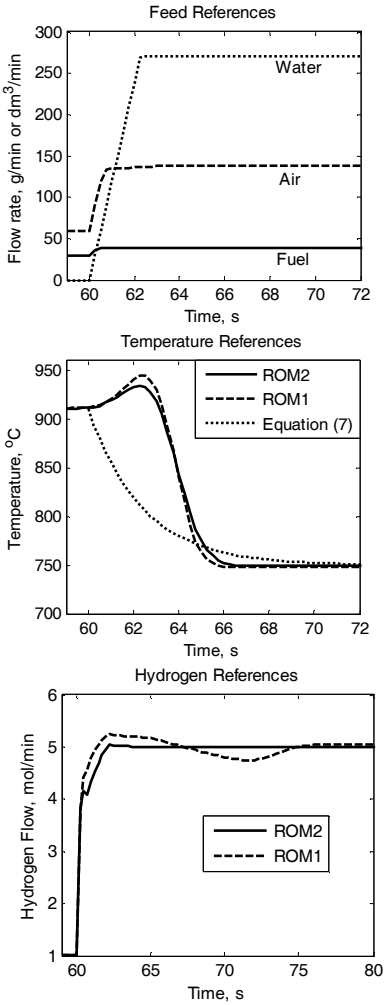

Figure 2: Calculated input & output references (top: feed flow rates; middle: reactor temperature, T_2; bottom: hydrogen flow)

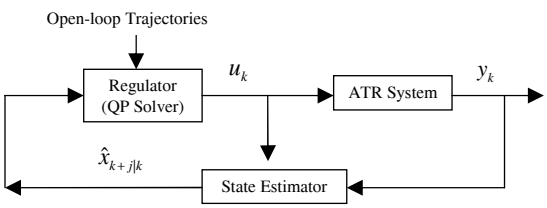

Figure 3: MPC structure: Receding horizon regulator & state estimator

V. Model Predictive Control

Once we have determined the reference trajectories, we can design the feedback portion of the predictive controller. The structure of proposed MPC is shown in figure 3 where the ATR system is simulated by ROM1 but the controller design is based on ROM2. The strategy used in this work is to develop a linear model which is successively linearized around the offline calculated trajectories, then formulate an unconstrained linear quadratic programming (QP) problem which can be solved within the sample time of the controller. However, the linear model used by MPC will suffer model mismatch due to modeling errors and unmeasured disturbances entering the system. In order to capture these errors, the Kalman Filter (KF) based state estimator is employed to reconstruct the system states from the available temperature measurements.

A. The Time-Varying Linear Model

In order to implement MPC online, we develop successive linear models around the input and output trajectories obtained in the previous section.

Starting from equation (9), $\hat{q}_d$ can be linearized around the trajectories as follows:

$$\hat{q}_d = \hat{q}_d\big|_r + B_k\tilde{u}_k + D_k\tilde{x}_k + E_k\tilde{g}_k \tag{11}$$

where $\tilde{u}_k = u_k - u_{r,k}$, $\tilde{x}_k = x_k - x_{r,k}$, $\tilde{g}_k = g_k - g_{r,k}$, $B_k = \left.\frac{\partial \hat{q}_d}{\partial u_k}\right|_r$, $D_k = \left.\frac{\partial \hat{q}_d}{\partial x_k}\right|_r$ and $E_k = \left.\frac{\partial \hat{q}_d}{\partial g_k}\right|_r$. Then, the linearization of equation (9) will lead to

$$\begin{aligned} \tilde{x}_{k+1} &= A_k\tilde{x}_k + B_k\tilde{u}_k + E_k\tilde{g}_k, \quad k = 0, 1, 2, \cdots \\ \tilde{y}_k &= C\tilde{x}_k \end{aligned} \tag{12}$$

where $\tilde{y}_k = y_k - y_{r,k}$ and $A_k = A_d + D_k$.

B. State Estimation

The state estimation algorithm with KF is based on the fact that the actual system always suffers various disturbances and noise. Using the combined input and output disturbance modeling procedure of [18], the following augmented linear model was developed:

$$\begin{aligned} z_{k+1} &= \mathbf{A}_k z_k + \mathbf{B}_k\tilde{u}_k + \mathbf{G}\xi_k, \quad k = 0, 1, 2, \cdots \\ y_k &= \mathbf{C}z_k + v_k \end{aligned} \tag{13}$$

where $z = \begin{bmatrix}\tilde{x} & \tilde{g} & p\end{bmatrix}^T$, $\xi = \begin{bmatrix}w & \omega & \upsilon\end{bmatrix}^T$ and the matrices $\mathbf{A}_k$, $\mathbf{B}_k$, $\mathbf{G}$ and $\mathbf{C}$ are appropriately defined. w, ω, υ, and v are white noise sequences with zero mean and covariance $Q_w, Q_\omega, Q_\upsilon$, and R_v respectively.

It has been indicated that, in order to make the augmented system detectable the combined number of states in the *g* and *p* vectors cannot be greater than the number of outputs [18]. For the ATR system, the number of states in the *p* vector is conservatively selected to be one because the system has 3 outputs (but only one controlled output) and the number of states in the *g* vector is one (this represents the inlet gas temperature).

Based on equation (13), the following KF is obtained:

$$\begin{aligned} \hat{z}_{k|k-1} &= \mathbf{A}_{k-1}\hat{z}_{k-1|k-1} + \mathbf{B}_{k-1}\tilde{u}_{k-1} \\ \hat{z}_{k+1|k} &= \mathbf{A}_k\hat{z}_{k|k-1} + \mathbf{B}_k\tilde{u}_k + \mathbf{L}_k(y_k^m - \mathbf{C}\hat{z}_{k|k-1}) \end{aligned} \tag{14}$$

where $\hat{z}_{k+1|k}$ is the estimate of the augmented state vector at time k+1 given output measurements up to time k; y_k^m is the measurement of y_k; the discrete Kalman filter gain, $\mathbf{L}_k$ is determined by the following recursive equations:

$$\begin{aligned} \mathbf{L}_k &= P_{k|k-1}\mathbf{C}^T(\mathbf{C}P_{k|k-1}\mathbf{C}^T + R_v)^{-1} \\ P_{k|k-1} &= \mathbf{A}_{k-1}P_{k-1|k-1}\mathbf{A}_{k-1}^T + \mathbf{G}\mathbf{Q}_\xi\mathbf{G}^T \\ P_{k|k} &= (I - \mathbf{L}_k\mathbf{C})P_{k|k-1} \end{aligned} \tag{15}$$

C. Control Formulation

To track the temperature reference trajectory determined by problem (10) and obtain the optimal control moves, the following quadratic objective function is used for the regulator.

$$\min_{u_i^j} J = \sum_{k=1}^{P}\beta\cdot\hat{y}_{c,k}^2 + \sum_{i=0}^{M-1}\sum_{j=1}^{3}\gamma^j\tilde{u}_i^{\,j} \tag{16}$$

where $\hat{y}_{c,k} = \hat{T}_{2,k} - T_{2r}$ and β, γ^j are weighting constants. The above minimization is typically subject to the following model equations and input magnitude, rate and output magnitude constraints:

$$\begin{aligned} z_{k+1} &= \mathbf{A}_k z_k + \mathbf{B}_k\tilde{u}_k + \mathbf{G}_\xi\xi_k \\ \hat{y}_{c,k} &= c_1(\mathbf{C}z_k + v_k) \end{aligned} \tag{17}$$

$$\begin{aligned} &\tilde{u}_i^{\,j,low} \le \tilde{u}_i^{\,j} \le \tilde{u}_i^{\,j,high}, \quad 0 \le i \le M-1 \\ &-\Delta\tilde{u}_i^{\,j,\max} \le \Delta\tilde{u}_i^{\,j} = \tilde{u}_i^{\,j} - \tilde{u}_{i-1}^{\,j} \le \Delta\tilde{u}_i^{\,j,\max}, \\ &y_{c,k}^{low} \le \hat{y}_{c,k} \le y_{c,k}^{high}, \quad 1 \le k \le P \end{aligned} \tag{18}$$

where $c_1 = [1 \quad 0 \quad 0]$. The above three equations formulate a classic QP problem which can be solved easily by the QP solver available in the literature. The simulations, however, show that it still costs around 15 seconds to solve equations (16) through (18) with appropriately small model and MPC parameters (N = 20, P = 10 and M = 5). So it is impossible to complete the required online calculations within a sampling time of the ATR system.

Recall that we have considered all process variable constraints indicated by equation (18) during the reference trajectory calculations, so those constraints are not likely to be violated during the closed-loop implementation. Hence, we propose to implement the unconstrained MPC problem. The advantage being that the solution may now be calculated analytically.

$$\mathbf{u}^* = K_1 d_1 \tag{19}$$

where K_1 is trajectory dependent matrix which can be evaluated off-line, rather than on-line, provided that the input and output trajectories are known. The only variable which

requires on-line computation is d_1 given by

$$d_1 = \begin{bmatrix} \mathbf{A}_k \hat{z}_{k|k-1} + \mathbf{L}_k (y_k^m - \mathbf{C}\hat{z}_{k|k-1}) \\ 0 \\ \vdots \\ 0 \end{bmatrix} \quad (20)$$

where y_k^m is the measurement of T_2 at time k. Thus, no solver with iterative methodologies is needed and the computational cost will be reduced sufficiently for on-line implementation.

VI. Simulation and Discussion

The multivariable MPC strategy of section V is tested under start-up conditions in the presence of system noise, inlet temperature and feedstock disturbances. The system noise is modeled as Gaussian white noise filtered through a linear system with transfer function $50/50s^3 + 20s^2 + 5s + 1$. This filtering allows for the capture of intermediate frequency disturbances, which are distinct from the mostly high frequency content of the measurement noise. The design parameters of the proposed KF based NMPC are chosen as follows:

$$\Delta T_s = 0.5s,\ N = 20,\ z_{0|0} = 0,\ P_{0|0} = \mathbf{I},\ Q_w = \alpha \mathbf{I},\ \alpha = 0.01,$$
$$Q_\omega = 0.25,\ Q_v = 14.5,\ R_v = 0.25\,\mathbf{I},\ \beta = 1,\ \gamma^j = 40,$$
$$w = 0.001,\ M = 5,\ P = 17$$

The selection of the control and prediction horizons is based on the guidelines presented in [17].

Figure 4 compares the simulation results from the open-loop, the feed-forward control and KF-based NMPC for start-up with an inlet temperature step disturbance, +20 ^oC. During this start-up, the fuel flow is increased from 30 to 38.2 g/min, the air flow is increased from 60 to 137.9 dm^3/min and the steam with a flow rate, 271.3 g/min is injected. As a result, the hydrogen flow for the start-up is expected to increase from 1 to 5 mol/min. The optimal trajectories determined in section 4 are used for the open loop case. The feed-forward controller developed in [8] is used for the feed-forward case where the fuel and steam flows follow the optimal references but the air flow is considered as the manipulated variable. The change of steam flow is considered as the disturbance. The PI controller parameters used are: $K_c = 0.15$, $T_I = 6.8$ and the parameters of feed-forward element used are: $K_f = 0.287$, $\tau_1 = 2.0$ and $\tau_2 = 1.6$.

As shown in the top plot of figure 4, the feed-forward controller causes an unacceptable drop in reactor temperature (~100 ^oC lower than the set-point of 750 ^oC) and would extinguish the reactor because the temperature is much lower than the temperature bound, 700 ^oC (see the dotted line). For the KF-based NMPC, we can see greatly improved performance because the temperature is well controlled and driven to the set-point within 7 seconds. It is also noted that the hydrogen flow, under the NMPC, shows a significant increase in variability (see the bottom plot of figure 5). However, we expect that a retuning of the NMPC will be able to reduce these variations.

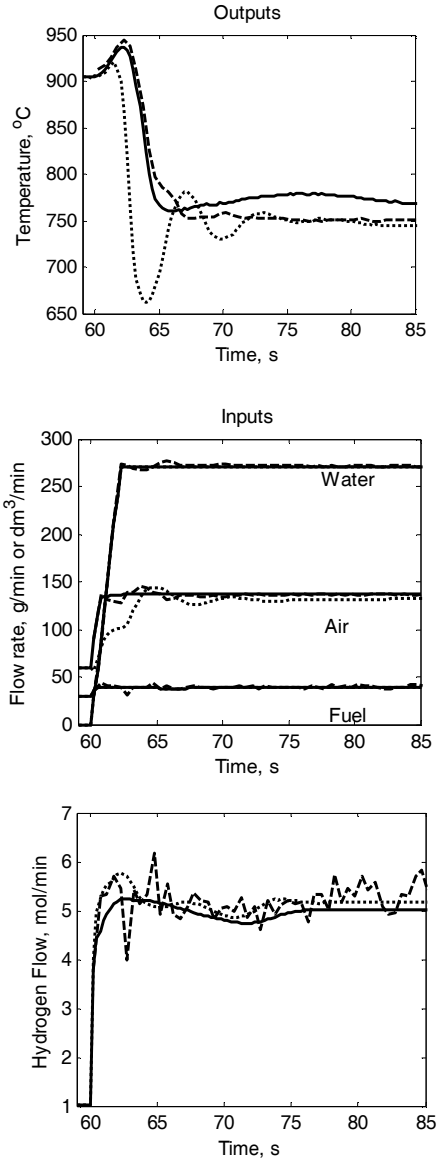

Figure 4: Response of open-loop (solid line), feed-forward control (dot line) and NMPC (dashed line) for inlet gas temperature disturbance

To test another model mismatch case, the feedstock is changed from gasoline ($C_{7.3}H_{14.28}$) to n-octane (C_8H_{18}). As shown in the top plot of figure 5, applying the open-loop input references will lead to a temperature drop of 45 ^oC, which means the plant is significantly different from the gasoline based ROM used in the controller. Once again, the feed-forward control shows poor performance because the temperature drops down to 640 ^oC which will again extinguish the reactor. The KF-based MPC shows excellent performance by adjusting the flow rate air (see the middle plot of figure 5). However, as shown in the bottom plot of figure 5, hydrogen production is reduced to ~4.5 mol/min, which is lower than the demand, 5 mol/min. For such

situations, the trajectories used by the MPC should be recalculated and updated with the new data. However, such calculations are not required frequently and can be conducted offline.

VII. Conclusion

In this work, we have proposed a KF based nonlinear multivariable predictive control structure aimed at regulating the temperature/hydrogen flow of an ATR reactor for onboard fuel processor applications while achieving the minimum fuel cost. In response to hydrogen demand, the optimal fuel, air and steam flows can be found through the analytical solutions developed. It was found that KF-based NMPC scheme is capable of sufficient disturbance attenuation through reconstruction of the system states as well as identification of input and measurement disturbances. The successive linearized model around the input and output trajectories can be effectively used for the nonlinear MPC and thus reduce the computation required. The simulations show that the KF based NMPC achieves good performance and can be implemented online. It should be cautioned that the reference trajectories used in this work are determined offline.

Acknowledgment

The authors wish to thank the Department of Chemical and Biological Engineering, and the Fieldhouse Fellowship Foundation, IIT for financial support.

References

[1] S. Ahmed and M. Krumpelt, Hydrogen from hydrocarbon fuels for fuel cells, *Int. J. Hydrogen Energy*, 26 (2001), 291.

[2] M. Pacheco, S. Jorge and J. Kopasz, Reaction kinetics and reactor modeling for fuel processing of liquid hydrocarbons to produce hydrogen: isooctane reforming, *Appl. Catal., A: Gen*., 250 (2003), 161.

[3] L. Villegas, N. Guilhaume, H. Provendier, C. Daniel, F. Masset and C. Mirodatos, A combined thermodynamic/experimental study for the optimization of hydrogen production by catalytic reforming of isooctane. *Appl. Catal., A: Gen*., 281(2004), 75.

[4] D. Trimm, A. Adesina, A. Praharso and N. Cant, The conversion of gasoline to hydrogen for on-board vehicle applications, *Catalyst Today*, 17(2004), 93.

[5] D. Papadias, S. Lee and D. Chmielewski, Autothermal reforming of gasoline for fuel cell applications: a transient reactor model, *Ind. Eng. Chem. Res*. 45(2006), 5841.

[6] H. Gorgun, M. Arcak, S. Varigonda and S. Bortoff, Nonlinear observer design for fuel processing reactors in fuel cell power systems, in: *Proc. of the 2004 Am. Cont. Conf*. (2004), p. 845.

[7] J.T. Pukrushpan, A.G. Stefanopoulou, S. Varigonda, L.M. Pedersen, S. Ghosh and H. Peng, Control of natural gas catalytic partial oxidation for hydrogen generation in fuel cell applications, *IEEE Trans. on Cont. Sys. Tech.*, 13(2005), 3.

[8] Y. Hu, D. Chmielewski and D. Papadias, Autothermal Reforming of Gasoline for Fuel Cell Applications: Controller Design and Analysis, *J. Power Sources*, 182 (2008), 298.

[9] S. Qin and T. Badgewell. A survey of industrial model predictive control technology, *Cont. Eng. Practice*, 11 (2003), 733.

[10] J. Rawlings, Tutorial: model predictive control technology, *proceedings of the American Control Conference*, June 1999, San Diego, CA, 662.

[11] B. Bequette, Nonlinear model predictive control: a personal retrospective, *The Can. J. of Chem. Eng*., 85(2007), 408.

[12] G. Gattu and E. Zafiriou, Nonlinear quadratic dynamic matrix control with state estimation, *Ind. Eng. Chem. Res*., 31(1992), 1096.

[13] J. Lee and N. Ricker, Extended Kalman filter based nonlinear model predictive control, *Ind. Eng. Chem. Res*., 33(1994), 1530.

[14] Y. Hu, D. Chmielewski and D. Papadias, Autothermal Reforming of Gasoline for Fuel Cell Applications: A Control-Oriented Dynamic Model, *Ind. Eng. Chem. Res*., 47(2008), 9437.

[15] S. Ahmed, R. Ahluwalia, S. Lee and S. Lottes, A gasoline fuel processor designed to study quick-start performance, *J. Power Sources*, 154(2006), 214.

[16] Z. Chen, S. Elnashaie, Optimization of reforming parameter and configuration for hydrogen production, *AIChE J*., 51(2005), 1467.

[17] D.E. Seborg, T.F. Edgar and D.A. Mellichamp, *Process Dynamics and Control*, second ed., John Wiley & Sons, Hoboken, NJ, 2004.

[18] K. R. Muske and J.B. Rawlings, Model predictive control with linear model, *AIChE J*., 39(1993), 262.

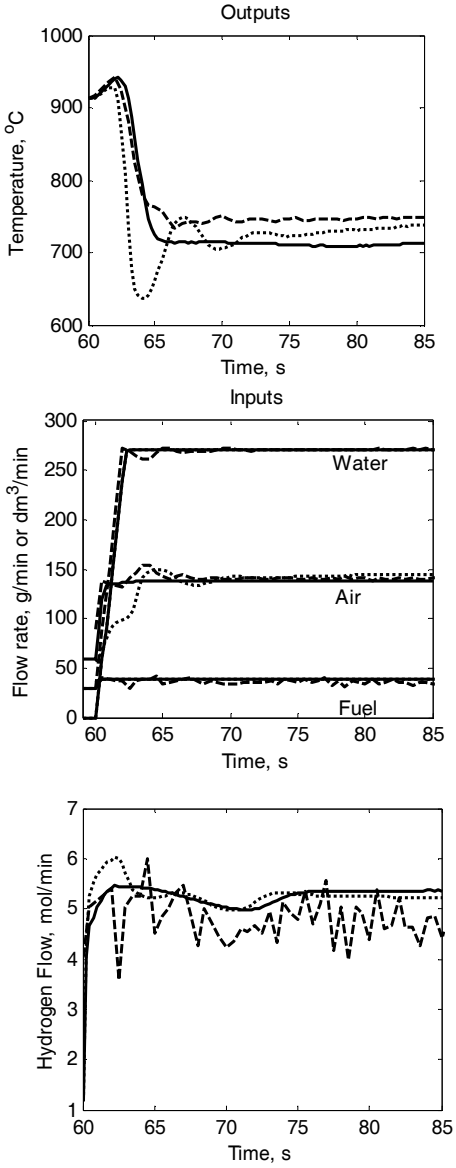

Figure 5: Response of open-loop (solid line), feed-forward control (dot line) and NMPC (dashed line) for feedstock mismatch